Edelweiss Applied Science and Technology
ISSN: 2576-8484
Vol. 9, No. 4, 379-394
2025
Publisher: Learning Gate
DOI: 10.55214/25768484.v9i4.5993

MGWO-CNN: A bio-inspired deep learning approach for COVID-19 detection in chest X-ray images

Roseline Oluwaseun Ogundokun[1*], Pius Adewale Owolawi[2], Chunling Du[3]
[1,2,3]Department of Computer Systems Engineering, Tshwane University of Technology (TUT), Pretoria, South Africa; ogundokunroseline1@gmail.com (R.O.O.).

Abstract: The present COVID-19 pandemic demands rapid and accurate diagnostic methods for early detection, isolation, and treatment. This study aims to enhance COVID-19 diagnosis with the help of bio-inspired deep learning and feature selection. This paper proposes a novel diagnostic model—MGWO-CNN—integrating a Modified Grey Wolf Optimizer (MGWO) with a Convolutional Neural Network (CNN). The framework utilizes Gabor filters as feature detectors and MGWO to optimize feature selection and improve classification performance. The model was tested and trained on a publicly available Kaggle dataset of 13,758 CXR images. Experimental results show that the MGWO-CNN outperforms traditional methods with 99.89% accuracy, 100% sensitivity, and 99.79% specificity. The model effectively distinguishes between COVID-19 and normal cases with significantly lower training and validation loss than baseline models. MGWO-CNN provides higher diagnostic accuracy, validating the effectiveness of bio-inspired optimization-based hybrid deep learning for COVID-19 diagnosis. The model offers an affordable, effective diagnostic tool that can be adopted in resource-constrained healthcare settings with limited access to high-end testing equipment.

Keywords: *Chest X-ray images, Convolutional neural network, COVID-19, Classification, Deep learning, Gabor filter, Greywolf optimizer algorithm.*

1. Introduction

COVID-19, a novel coronavirus, emerged late in 2019 and quickly spread from Asia to the rest of the world, producing an unforeseen global epidemic of respiratory diseases [1, 2]. The emergence of COVID-19 has had profound economic repercussions and continues to pose a substantial risk to human life [3]. The global dissemination of the epidemic has resulted in a cumulative count of about 36 million confirmed illnesses and 1 million documented fatalities globally [4]. Numerous study initiatives have been conducted to assess the extent and gravity of pneumonia induced by COVID-19 within this time frame. The objective of these investigations is to efficiently identify individuals who have been infected with COVID-19 at the earliest feasible stage. It is crucial to isolate these patients promptly and minimize the risk of transmission while also ensuring that they get appropriate medical intervention [5, 6]. While chest X-ray (CXR) is widely available in hospitals globally, it is essential to note that chest computed tomography (CT) scans exhibit greater sensitivity compared to CXR in the early identification of COVID-19 disease alterations, as well as in the assessment of disease stage and monitoring of disease progression [7, 8]. Computed tomography (CT) images are generally recognized as a robust analytical technique [9, 10]. That finds extensive applications in the field of biomedical imaging Ye, et al. [11] and clinical diagnostics [12]. These images provide non-invasive three-dimensional visualization of inside structures, allowing detailed examination without causing any damage. Nevertheless, classifying the symptoms of community-acquired bacterial pneumonia becomes

History: Received: 13 January 2025; Revised: 19 March 2025; Accepted: 24 March 2025; Published: 5 April 2025
* Correspondence: ogundokunroseline1@gmail.com

challenging compared to COVID-19 [13]. Various studies [14-22]. Utilize different feature selection and extraction methods to improve their recommended systems' performance.

In contemporary times, evaluating vast data sets has become much more convenient owing to the emergence of the deep learning (DL) technique. CNN-centred DL procedure models are often considered the most favoured DL technique in medicine [23]. When educated about early diagnosis, patients can receive improved medical care and more tailored therapeutic interventions [24]. CNNs are a kind of artificial neural network (ANN) that falls under ML strategies. Recently, several CNN models have been widely utilized for image classification tasks. Notable examples are GoogLeNet Zhou, et al. [25] VGGNet Gupta and Bibhu [26] ResNet Lu, et al. [27] and AlexNet Dey and Rajinikanth [28]. Kassem, et al. [29] proposed a comprehensive examination of contemporary CNN architectures to recognize COVID-19 situations from non-COVID cases. Based on the studies, it has been seen that using deep learning methods in conjunction with radiograph pictures has promised a viable approach to identifying COVID-19. Much research focused on diagnosing COVID-19 using DL approaches mainly uses CNNs, as the literature reviewed in the Related Works section shows. CNNs can acquire localized temporal or geographical input responses. However, they are limited in their capacity to learn sequential connections.

The efficacy of existing approaches in advancing DL algorithms is a significant challenge. Given the criticality of precision in intelligent medical systems, an exact model has been developed to tackle this issue effectively. The study proposed using a Modified Greywolf Optimizer Algorithm Fu, et al. [9] in conjunction with CNN (MGWO-CNN) to analyze chest X-ray images. Image characteristics are often created using automated DL algorithms.

The research focused on deep learning processes as a significant visual separation tool that has emerged in recent years. CNN has achieved tremendous progress in digital image learning activities [30]. The need for human removal of features by image alteration or encryption techniques has been prevented by the advent of CNNs, which provide an integrated and automated solution for rendering and feature extraction. Consequently, diverse, comprehensive cognitive approaches rooted in DL have been developed. This study aims to assess the accuracy of a combination approach, including the MGWO algorithm and CNN, for feature categorization. Using both transfer functions, as opposed to just one, enhances the efficacy of the algorithm under consideration.

Furthermore, the relevant parameters Eldred-Evans, et al. [31] for updating the attributes throughout the exploration of MGWO or CNN have been meticulously chosen, as shown by the experiments. Datasets characterized by a high dimensionality exhibit a diminished level of accuracy in their categorization. Identifying and selecting the most informative and valuable characteristics from chest X-ray datasets is often called feature selection (FS). The use of this technique serves to improve the precision of predictions and decrease the number of attributes involved. The core objective of the presented approach is to advance the efficacy of the feature selection (FS) methodology [32]. This research offers a novel approach that utilizes a modified Grey Wolf Optimization (MGWO) strategy in conjunction with CNN to decrease the number of features and accurately diagnose COVID.

The core contributions of this study are summarized as given below:

a. A modified Greywolf Optimizer (MGWO) algorithm
b. The MGWO optimization algorithm was used to tune CNN's hyperparameters.
c. A comprehensive comparison study is conducted to establish the effectiveness of the recommended method by comparing the optimized and un-optimized CNN.

The successive sections of the article are organized subsequently. Section 2 delivers a summary of the existing investigations on the COVID-19 pandemic. The approach and dataset are discussed in Section 3. The assessment of performance and the corresponding outcomes are obtainable in Section 4. The research findings are discussed in Section 5, compared with earlier research. Chapter 6 serves as the concluding section of the essay, offering insights into potential future endeavours.

Edelweiss Applied Science and Technology
ISSN: 2576-8484
Vol. 9, No. 4: 379-394, 2025
DOI: 10.55214/25768484.v9i4.5993

2. Related Works

Within the realm of literature, several studies have been conducted on utilizing Artificial Intelligence (AI) for a range of objectives, including the detection of Alzheimer's illness, estimate of cancer, analysis of biopsies, and examination of dermoscopy, among others [31-38]. In contemporary times, the COVID-19 epidemic has significantly burdened healthcare professionals. Consequently, the assistance provided by artificial intelligence to doctors enhances the efficacy and soundness of their jobs and decision-making processes. In the present context, scholarly literature presents a range of methodologies that have been suggested for the interpretation of X-ray or CT pictures for COVID-19. Several prior investigations may be briefly described as follows:

Khan and Aslam Ucar and Korkmaz [39] introduced a diagnostic tool that utilizes DL algorithms to assist in identifying COVID-19 by analysing X-ray pictures. The present research examined a selection of DL approaches. Conferring to the research, the VGG-16 and VGG-19 models exhibit superior performance compared to other versions. In a study by Jaiswal and Bist [40] X-ray pictures were used to recognize COVID-19 by implementing diverse DL techniques. The research included a comparison of the performances of several CNN architectures.

Furthermore, the proposal to implement a majority rule was an innovative strategy. The highest recorded effectiveness in the article was reported as 98.96%. Nour, et al. [35] introduced a CNN architecture as an automated diagnostic method for recognising positive COVID-19 cases using X-ray pictures. The presented CNN model, which comprises a serial network with five convolutional layers, was trained starting with the initial weights and the CNN model was utilized to retrieve distinctive characteristics.

According to the findings, the SVM classifier demonstrated the highest efficiency level, ensuring optimal outcomes with an accuracy rate of 98.97%. Chowdhury, et al. [36] recommended a deep CNN-based transfer learning (TL) method for the automated identification of COVID-19 pneumonia via the analysis of X-ray pictures. Eight well-recognized CNN-based DL algorithms were used for training, including SqueezeNet, ResNet18, InceptionV3, and others. The DenseNet model had the most incredible classification success rate of 97.94% in research consisting of three classes and using data augmentation techniques. Asif, et al. [37] introduced DCNN to automate the diagnosis of COVID-19 via the analysis of X-ray images. The X-ray pictures were used in a DCNN-founded approach, Inception-V3, using TL techniques lacking preprocessing steps. The diagnostic procedure had a classification accuracy of 96%.

Toğaçar, et al. [38] utilized a deep learning (DL) approach to identify COVID-19 by analyzing X-ray images. Their study involved a preprocessing step where class structures were refined using a fuzzy color technique. The original images were combined with structured visuals to create a multi-layered dataset, which was then processed using MobileNetV2 and SqueezeNet deep learning models. An SVM model was employed for classification, achieving an accuracy of 99.27%.

Similarly, MUcar and Korkmaz [39] developed an artificial intelligence (AI) system for detecting COVID-19 in chest X-rays. They enhanced the dataset through augmentation and optimized the SqueezeNet framework using Bayesian optimization, resulting in a classification accuracy of 98.3%.

In another study, Ozturk, et al. [41] introduced an automated DL approach for COVID-19 detection using the DarkCovidNet model. Unlike other studies, their method did not incorporate preprocessing steps such as augmentation or segmentation. Despite this, their model achieved an accuracy of 87.02% when classifying data into three categories.

Furthermore, Khan and Aslam [34] designed CoroNet, a CNN model for COVID-19 detection using CT and X-ray images. Based on the Xception architecture and pretrained on the ImageNet dataset, CoroNet demonstrated effective performance in distinguishing COVID-19 cases.

In the study, Canayaz, et al. [42] proposed a new approach integrating BO with MobileNetV2 and ResNet-50 models, along with SVM and kNN algorithms. The approach achieved an accuracy of 99.37%. Mean precision, recall, and F1-score were 99.38%, 99.36%, and 99.37%, respectively, for all COVID-19 and non-COVID-19 class datasets. Based on the performance measures, the proposed

Edelweiss Applied Science and Technology
ISSN: 2576-8484
Vol. 9, No. 4: 379-394, 2025
DOI: 10.55214/25768484.v9i4.5993

method is highly effective. It can be used as a decision-support system to diagnose COVID-19 effectively from CT scans.

Junia and Selvan [43] presented the Ensemble Neural Net Sentinel Algorithm (ENNSA), an innovative deep learning (DL) method proposed explicitly for segmentation and classification of COVID-19. The study applied a chest X-ray dataset extracted from Kaggle, which was first preprocessed before feature extraction using the Insistent Grey Level Co-occurrence Matrix (IGLCM). The constructed ENNSA performed better than other approaches in accuracy, precision, recall, and F1-score, being 99.25%, 100%, 43%, and 61%, respectively, including when tested on imbalanced data. These facts support its robustness as a guaranteed diagnosis tool for respiratory infections. The segmentation mechanism adopted in this research effectively identified important features from chest X-ray images utilized to classify COVID-19. Experimental results confirm that the ENNSA model outperforms conventional techniques in accurately diagnosing COVID-19 cases.

Kong, et al. [44] proposed an Edge Computing-based Mask Identification Framework (ECMask) to support public health measures by enabling real-time mask detection on low-power camera equipment, e.g., installed on buses. The ECMask system has three major phases: (1) restoration of video, (2) face detection, and (3) mask recognition. The models used at each stage were trained and validated on a combination of a private bus drive monitoring dataset and available public datasets. Exhaustive experiments with real-world video data were conducted to measure the detection accuracy and time complexity of execution of the new framework. The results confirm that ECMask functions well in actual settings, toward its promising application as an instrumental aid for COVID-19 prevention and public health surveillance.

Dash and Swarnkar [45] explored the use of Generative Adversarial Networks (GANs) for data augmentation to improve training data for deep learning models for disease detection, including COVID-19 diagnosis using chest X-ray (CXR) images. DCGAN and Vanilla GAN approaches were employed in the research for data augmentation to address data paucity challenges. These generated images were evaluated using an ensemble deep learning model from VGG16, ResNet50, DenseNet, and LSTM. The method has produced incredible results, i.e., detection rate 98%, sensitivity 99%, and specificity 100%, compared to the models trained on real data alone. The assessment metrics, such as precision, recall, F1-score, 11.685 PSNR and 0.598 SSIM, also supported the usability and quality of synthetic data. It is evident that the effectiveness of GAN-based augmentation towards the enhancement of CXR image classification for COVID-19 is showcased, and future research work and the optimization of the architecture of the GANs in medical imaging tasks are outlined.

2.1. Motivation, Novelty and Contribution

Despite using CNN in the state-of-the-art approaches, these methods fail to consider the spatial interdependence among picture pixels during model training. Therefore, when the pictures undergo rotation, specific resizing procedures, and data augmentation, which is necessary owing to the dataset's small scope, the generated CNN models exhibit inaccuracies in reliably identifying instances of COVID-19, viral pneumonia, and regular chest X-ray scans. While it is acceptable to have some level of misclassification in the identification of viral pneumonia patients, misclassifying instances of COVID-19 as typical or viral pneumonia might have a detrimental impact on the therapy doctors administer.

The present study seeks to overcome the abovementioned constraints by creating an automated diagnostic process for screening individuals with COVID-19 using chest X-ray images. The approach described in this study utilizes an optimal and resilient CNN architecture to categorize chest X-ray pictures into three distinct classes. The suggested work exhibits dual originality. The mechanism used for tuning the hyperparameters of the CNN is distinctive. The hyperparameters of CNNs are optimized using MGWO. The hyperparameter tuning process included using a COVID-19 dataset for training, validation, and testing. The trial yielded favourable performance metrics.

Edelweiss Applied Science and Technology
ISSN: 2576-8484
Vol. 9, No. 4: 379-394, 2025
DOI: 10.55214/25768484.v9i4.5993

3. Materials and Methods

Isolating COVID-19 images from chest radiographs plays a crucial role in diagnostics. The proposed MGWO algorithm, integrated with a CNN, enhances classification accuracy by minimizing computational complexity and improving processing efficiency. Computer-assisted diagnosis of COVID-19 through chest X-ray image analysis has gained significant attention.

As highlighted earlier, this approach involves three key stages. The study primarily explores preprocessing, FE, FS, and classification techniques utilized in the MGWO-CNN model. Figure 1 illustrates the block diagram of the proposed methodology. The framework employs a Gabor filter to extract distinguishing features from chest X-ray images. The extracted features are then refined by combining the MGWO and CNN algorithms, ensuring optimal feature selection. Transmission experiments were conducted to enhance the differentiation of chest X-ray images, further improving diagnostic accuracy.

3.1. Dataset Collection

The dataset for COVID-19, consisting of 13,758 scans, was acquired from the Kaggle repository. The dataset may be retrieved using the succeeding link: https://www.kaggle.com/tawsifurrahman/covid19-radiography-database (Accessed July 7th, 2023). There are three chest X-ray images: normal, COVID-19, and others. A total of 3,617 photos depicting cases of covid-19 and 10,141 photographs representing typical cases were involved in the dataset. Specifically, 80% of the dataset was assigned for the training task. In contrast, the remaining 20% was set aside for testing.

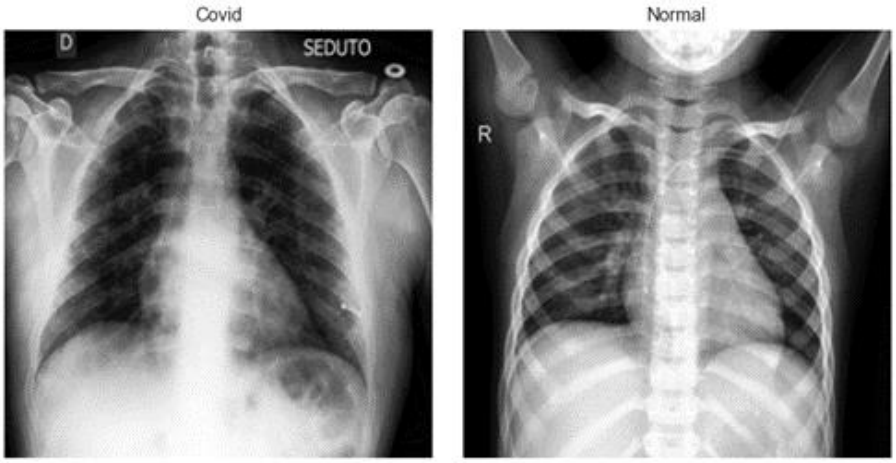

Figure 1.
Sample Dataset.

3.2. Methods

3.2.1. Feature Extraction (FE) using Gabor Filter

The Gabor filter exhibits high sensitivity towards structural elements and patterns, resulting in diverse responses when applied to a picture. The Gabor filter Kong, et al. [44] is utilized to eliminate the image element due to its optimal positioning for frequency and temporal localization. The Gabor function is mathematically described in a two-dimensional space according to Equation (1).

$$G(x_1, y_1, \lambda, \theta, \emptyset, \sigma, \alpha) = e^{\frac{x1^2 + y^2 y^1}{2\sigma^2}} * \ e^{\beta} \ (2\Pi \frac{x1}{\lambda} + \ \Psi) \quad (1)$$

Edelweiss Applied Science and Technology
ISSN: 2576-8484
Vol. 9, No. 4: 379-394, 2025
DOI: 10.55214/25768484.v9i4.5993

Where, $x_1 = xcos(\pi) + ysin(\pi)$ and $y_1 = -xcos(\pi) + ysin(\pi), \lambda$ = Bandwidth of the function, π = Symmetry of Gabor filter sinusoidal signal and phase offset α = Aspect ratio of space σ = Exponential envelope standard error are specified respectively. The use of a mathematical approach quantitatively characterizes the texture of the picture. Biomedical images are classified based on their mathematical attributes. The Gray-Level Co-occurrence Matrix (GLCM) is a procedure that may be used to quantify the occurrence of two pixels at a certain distance from each other.

The recommended technique involves variations in both the wavelength and structure of the Gabor filter. The frequencies often seen are 3.0 and 0.6, whereas the average orientations are distributed at five specific angles: 0, 45, 90, 135, and 180. Consequently, there are a total of 10 potential combinations. The statistical determination of picture elements occurs after the image has been transferred to the Gabor filters, which consist of five statistical characteristics and ten different filters.

3.2.2. Convolutional Neural Network

CNN is a type of ANN designed for image recognition and segmentation. CNN demonstrates a high level of proficiency in recording the intricate attributes of the re-lease phase. The evaluation of CNN may include an assessment of bias and the consideration of weighted neurons. Every individual neuron inside a neural network is subjected to a unique input and afterwards selects the information with the most incredible value to serve as the active function. The extraction of a significant proportion of the size of a feature in a CNN is achieved via a sequence of convolutional layers and an indirect Rectified Linear Unit (ReLU) function [45]. The maximum pooling layer is used in the reduction factor map. Every neuron inside the system is connected to every other neuron in the pre-dense compression layer, forming a fully integrated network. Backpropagation and gradient shrinking are often used techniques in network training. The softmax function is a probability distribution often used to constrain the aggregate output of a class within the range of 0 to 1. At the concealed layer level, the Convolutional Neural Network (CNN) produces feature maps that assist the computational model in acquiring knowledge about minute visual characteristics.

The model is trained on identical MGWO and CNN parameter values inside a COVID-19 chest x-ray dataset. The use of a Gabor filter is employed throughout the process of algorithm creation. The task involves analyzing input chest X-ray data and evaluating the training process using an 80:20 ratio. Each chest X-ray image will be as-signed a label during the training phase. Subsequently, it is necessary to provide models for the input and output layers. The input convolution layer is produced by the output of FC8, which is subjected to 48 filters with 3*3 and 64 dimensions. Next, the activation function is applied to the CNN methodology, which is trained using the re-quired attributes for COVID-19 imaging. The algorithm for the suggested system, MGWO-CNN, is shown below.

Figure 2 depicts the proposed system, whereby a Gabor Filter is employed to enhance the efficacy and robustness of the methodology. Subsequently, the FS process is used to ascertain the greatest significant characteristics based on the given data, specifically in the context of MGWO-CNN.

Edelweiss Applied Science and Technology
ISSN: 2576-8484
Vol. 9, No. 4: 379-394, 2025
DOI: 10.55214/25768484.v9i4.5993

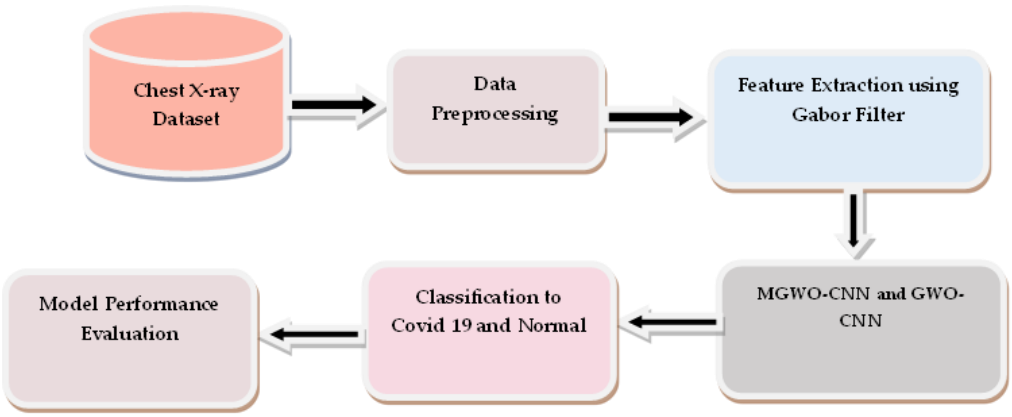

Figure 2.
Flow Diagram of the Proposed System.

3.2.3. Greywolf Optimization Algorithm

The GWO method belongs to the category of swarm-intelligence optimization algorithms, and its design has been affected by several instances. Mirjalili, et al. [46] proposed the simulation of grey wolves' hunting process as the Gray Wolf Optimizer (GWO). Grey wolves have a strictly hierarchical social structure, whereby an alpha wolf assumes the role of the primary decision-maker, with beta and delta wolves occupying subordinate positions. The set that remains is categorized as omegas, as stated by Mirjalili, et al. [46] in 2014.

The GWO technique is an optimization approach rooted in nature, which employs a hierarchical leadership structure to provide the most optimal solution to a given issue. Alpha wolves assume leadership roles within their pack and possess decision-making authority on hunting activities. The dominant wolves within the group consistently exhibit superior strength, exerting influence over decision-making processes, which necessitates compliance from the rest of the pack. The alpha members of a pack do not necessarily need to possess the highest level of physical strength. Still, they are more advantageous in exerting authority over the whole pack. The beta wolves have a subordinate position in social order. A beta wolf assumes the function of an alpha counselor, providing guidance and support to individuals in navigating their moral decision-making processes. The beta wolf takes the function of the alpha wolf upon the death or aging of the current alpha wolf. Omega wolves, who assume the role of the goat emissary, are responsible for enforcing the directives of the alpha inside the pack. Their primary function is to uphold law and order among all subordinate levels within the hierarchical structure that they oversee. Individuals are expected to submit to the dominant wolves, after which they participate in the act of consumption. The number of wolves, iterations, and population level are initialized during the preprocessing phase. By using this initialization, we may make estimations for the parameters α, β, δ, and ω. Wolves characterized by alpha, beta, delta, and omega attributes were considered socially acceptable.

The wolves' observed behaviour included encircling, which was quantified utilizing Equations (2) and (3).

$$\vec{D} = \left| \vec{C}.\overrightarrow{X_p}(t) - \vec{X}(t) \right|, \quad (2)$$

$$\vec{X}(t+1) = \overrightarrow{X_p}(t) - (\vec{A}\vec{D}), \quad (3)$$

In the above context, the symbol X denotes the representation of the wolf, while the symbol t represents the iteration. Additionally, X_p signifies the location of the moving target. The symbols A and C are provided in Equations (4) and (5) as follows.

The Global Wolf Organization (GWO) has developed many wolf specimens tasked with conducting targeted searches inside their territories. The wolves were assigned a specific region within which they

Edelweiss Applied Science and Technology
ISSN: 2576-8484
Vol. 9, No. 4: 379-394, 2025
DOI: 10.55214/25768484.v9i4.5993

were required to locate the target. The movement occurs when the values of j and k increase. The observed value of L exhibited increased as the candidate wolf approached the objective. The vectors $\vec{r}$ and $\overrightarrow{r_2}$ denote the directional movement of the wolf in pursuit of prey, optimizing the fitness function. The simulation included the manipulation of parameters to imitate the act of attacking prey. The components of a were systematically decreased linearly from a value of two to zero throughout several repetitions. The parameters as mentioned earlier, were then used in the computation of the Peak Signal-to-Noise Ratio (PSNR) value, utilizing the most optimal method for target identification.

$$\vec{A} = 2\vec{a} \,.\vec{r} - a \quad (4)$$

$$\vec{C} = 2\overrightarrow{r_2} \quad (5)$$

Subsequently, the PSNR was calculated employing the Mean Squared Error (MSE), with the formulae below:

$$MSE = \frac{1}{M \times N} \sum_{i=1} M \sum_{j=1} N(I(i,j) - J(j,i))^2) \quad (6)$$

$$PSNR = 10\log_{10}(\frac{{MAX_i}^2}{MSE}) \quad (7)$$

Equations (6) and (7) include the variables I, J, M, and N, which represent the original picture, the noisy image, and the dimensions of the image, respectively. In Equation (3), the symbol MAX_i denotes the maximum pixel value. The wolf location was established and then adjusted by identifying the highest PSNR value during the iteration. This process finally facilitated the localization of potential nodules. The procedure was iteratively executed until the optimal location of the wolf was attained across all initial populations of wolves.

Algorithm 1. Traditional grey Wolf Optimizer

Start

Step 1: Initiate the parameters maximum number of iterations, population size, dimension, higher bound and lower bound;

Step 2: Choose the starting locations of grey wolves with higher bound and lower bound;

Step 3: Initiate $\overrightarrow{X}_1, \overrightarrow{X}_2, \overrightarrow{X}_3$;

Step 4: Determine each grey wolf's fitness;

Alpha = highest fitness grey wolf;

Beta = second highest fitness grey wolf;

Gamma = third highest fitness grey wolf;

Step 5: While C is < maximum number of iterations

For i = 1: population size

Update the present location of the grey wolf in equation 9 above for traditional;

End for

Update $\overrightarrow{X}_1, \overrightarrow{X}_2, \overrightarrow{X}_3$

Determine the best fitness of the grey wolves;

D += D;

End while

Step 6: Return alpha;

End

Source: Hu, et al. [47].

3.2.4. Proposed MGWO-CNN Technique

This section provides an in-depth overview of the method we have recommended for categorizing chest X-ray pictures, referred to as the Modified Grey Wolf Optimization Convolutional Neural Network (MGWO-CNN). To provide more transparency, the suggested resolution has been broken down into phases as follows: (1) To begin, we present the MGWO-based technique, more precisely the MGWO technique, which effectively addressed the problems relating to prior image-noise reduction techniques, especially premature convergence towards the local optimal result. This is done by introducing the MGWO-based methodology. (2) Following this, the MGWO approach was implemented as a filtering procedure to locate the subset of characteristics that proved the most effective in identifying COVID-19 utilizing chest X-ray images. The MGWO technique, as stated by CNN, was established to examine the best practicable set of features to optimize the classification efficacy of the CNN classifier. This evaluation aimed to determine which set of features would prove best performing. To train the Convolutional Neural Network (CNN) classifier, an optimum subset of features was found by using the Multi-Objective Grey Wolf Optimizer (MGWO) method. These features were used in the training process.

Edelweiss Applied Science and Technology
ISSN: 2576-8484
Vol. 9, No. 4: 379-394, 2025
DOI: 10.55214/25768484.v9i4.5993

Algorithm 2. Modified grey Wolf Optimizer

Start

Step 1: Initiate the parameters maximum number of iterations, population size, dimension, higher bound and lower bound;

Step 2: Choose the starting locations of grey wolves with higher bound and lower bound;

Step 3: Initiate $\overrightarrow{W}$, $\vec{X}$, $\vec{Y}$ and $\vec{Z}$;

Step 4: Determine each grey wolf's fitness;

Alpha $\overrightarrow{W}$ = highest fitness grey wolf;

Beta $\vec{X}$ = second highest fitness grey wolf;

Gamma $\vec{Y}$ = third highest fitness grey wolf;

Delta $\vec{Z}$ = fourth highest fitness grey wolf;

Step 5: While C is < maximum number of iterations

For i = 1: population size

Update the present location of the grey wolf in equation 11 above for modified;

End for

Update $\overrightarrow{W}$, $\vec{X}$, $\vec{Y}$ and $\vec{Z}$;

Determine the best fitness of the grey wolves;

C += C;

End while

Step 6: Return alpha;

End

3.3. Preprocessing Stage

The first step included using Gabor filters for FE on the chest X-ray images. This was followed by implementing adaptive filtering utilizing the MGWO approach. The MGWO methodology is a nature-inspired technique that aims to identify the most efficient means of achieving the desired objective. To achieve precise goals within our scans or dataset, the MGWO was used. There are 3,617 photos related to the COVID-19 virus and 10,141 photographs classified as usual. The dataset was partitioned into two subsets, namely the training set and the testing set, with a ratio of 80:20. The dataset was divided into two halves, with 80% of the data allocated for the training job and the remaining 20% reserved for testing purposes.

Edelweiss Applied Science and Technology
ISSN: 2576-8484
Vol. 9, No. 4: 379-394, 2025
DOI: 10.55214/25768484.v9i4.5993

4. Results and Discussion

4.1. Experimental Configuration

The trials were conducted using a Dell Inc. 1.20.3 system with an Intel® Core™ i7-6600U processor operating at a frequency of 2.60GHz and a clock speed of 2801 Mhz. The system has 16.0 GB of physical memory and 16 GB of RAM. Additionally, the system is running the Anaconda 3 software environment. The device has a central processing unit (CPU) manufactured by Dell Inc., specifically version 1.20.3. After examining two distinct models, it was determined that the unique technique known as the MGWO-CNN model exhibited superior performance, achieving maximum accuracy. The training process for this model was completed within a few minutes using the specified configuration. The findings were obtained using Python programming language and OpenCV computer vision library. The model was tested using Scikit-learn and NumPy.

4.2. Results from Experimentation

The proposed research used the GWO and a CNN approach to assess its effectiveness in COVID-19 detection. Additionally, the study compared the performance of this approach to a novel modified GWO strategy that was recommended. The assessment dataset included 13,758 chest X-ray scans, 3,617 images depicting COVID-19 cases and 10,141 images representing normal cases. The performance and compilation time of the GWO-CNN model were assessed alongside the recommended MGWO-CNN model since the study goal is to determine the most optimal model. Each model was subjected to fine-tuning, including training for 50 epochs and using optimizers recommended by grid search. This fine-tuning process aimed at maximizing the loss function, employing a learning rate 0.0001. Before being processed by the neural network, the images underwent a downsampling procedure to achieve the required dimensions of 224×224, as specified by the models. Figure 1 presents a collection of chest radiographs, showcasing examples of both COVID-19 and normal cases. The preprocessed images were fed into the CNN models to enhance classification accuracy.

Initially, a validation set consisting of 10% of the training data was used as the default. The accuracy and loss values obtained during the training and validation phases were subsequently applied to the dataset for performance evaluation. The effectiveness of the proposed approach was assessed by computing the classification accuracy scores for both the training and validation stages. Figure 3 illustrates the accuracy scores recorded over 50 training epochs. The results indicate that the MGWO-CNN model outperformed other approaches, achieving a training accuracy of 96% and a validation accuracy of 99%. Similarly, the GWO-CNN model demonstrated a strong performance, attaining accuracy rates of 92% for training and 95% for validation.

The loss values of the models, which reflect their performance after each iteration, were also analyzed. A decrease in loss generally corresponds to improved model performance, provided overfitting does not occur. Figure 4 visualizes and quantifies the loss incurred during the training and testing phases. The results indicate a downward trend in average loss as the number of epochs increased. However, the extent of reduction varied across models. The MGWO-CNN model demonstrated superior performance, exhibiting significantly lower loss rates compared to the GWO-CNN model. Specifically, the MGWO-CNN model recorded a training loss of 11.28% and a validation loss of 4.73%, whereas the GWO-CNN model showed higher loss rates of 26.62% for training and 18.57% for validation. These findings confirm the effectiveness of the MGWO-CNN model in achieving improved classification performance.

Edelweiss Applied Science and Technology
ISSN: 2576-8484
Vol. 9, No. 4: 379-394, 2025
DOI: 10.55214/25768484.v9i4.5993

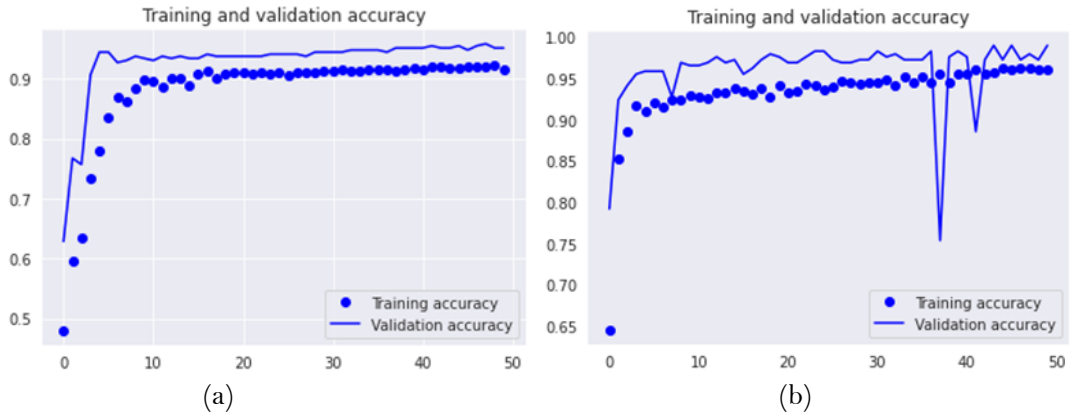

(a) (b)

Figure 3.
a. GWO-CNN and b. MGWO-CNN Training and Validation Accuracy Graph.

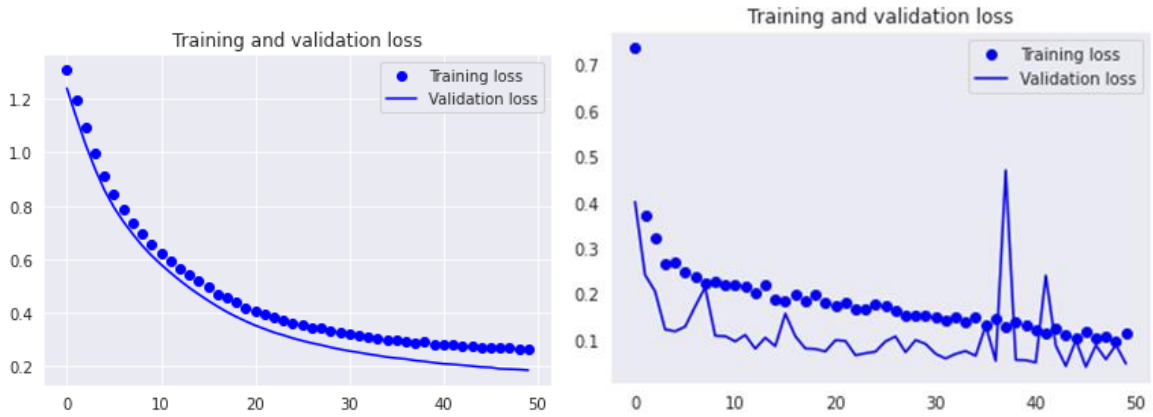

(a) (b)

Figure 4.
a. GWO-CNN and b. MGWO-CNN Model Entropy Graph.

Edelweiss Applied Science and Technology
ISSN: 2576-8484
Vol. 9, No. 4: 379-394, 2025
DOI: 10.55214/25768484.v9i4.5993

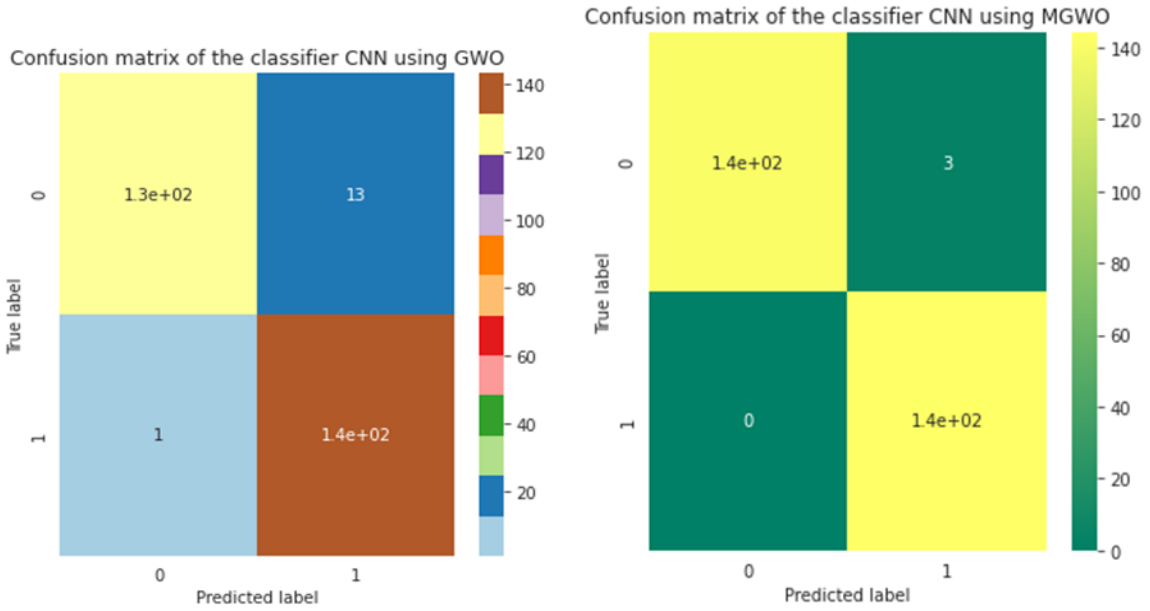

(a) (b)

Figure 5.
Confusion Matrix of the Models.

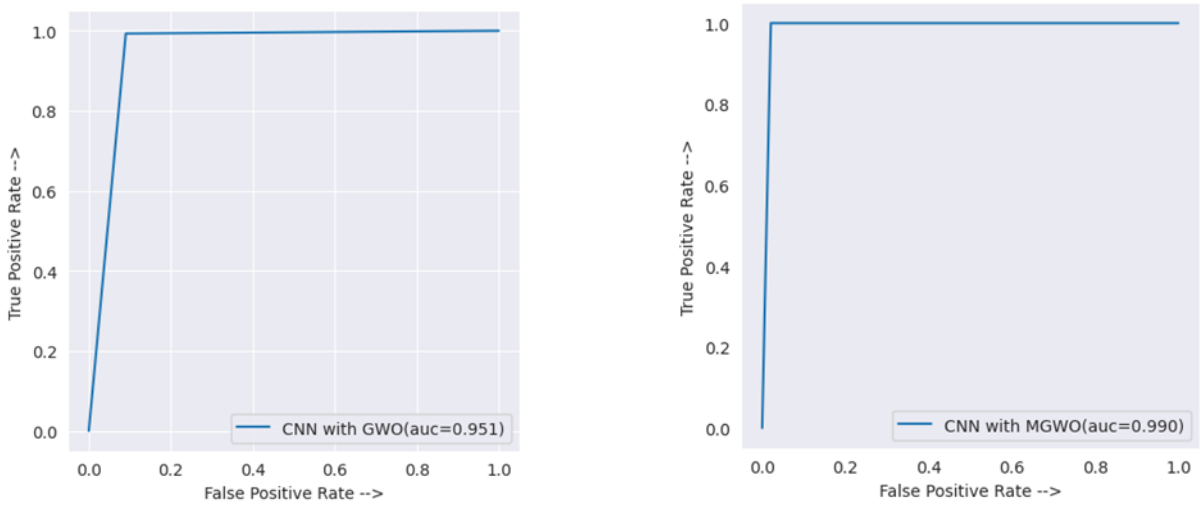

(a) (b)

Figure 6.
ROC-AUC Curve of the Model.

Figure 5 displays the confusion matrix for the models, serving as a visual representation to facilitate the assessment of their overall performance. The test dataset has 724 photos depicting cases of covid-19 and 2028 images representing normal cases. The matrix demonstrates that MGWO-CNN has effectively identified 1400 normal and 1400 Covid-19 samples. The model showed high accuracy, correctly identifying 99.89% of the data samples in the test set. Similarly, the GWO-CNN models demonstrated high accuracy by correctly classifying 1300 Covid-19 samples and 1400 healthy patients, resulting in an accurate rate of 99.48%. The labels TP, TN, FP, and FN values were calculated using the confusion matrix demonstrated in Figure 5. The equation (1) to (5) was employed to examine the

Edelweiss Applied Science and Technology
ISSN: 2576-8484
Vol. 9, No. 4: 379-394, 2025
DOI: 10.55214/25768484.v9i4.5993

effectiveness of the recommended system. The calculated values for the performance measures are obtainable in Table I. According to the data shown in the table, it is evident that the updated MGWO-CNN exhibits superior performance across several metrics. Notably, it achieves a precision score of 99.79%, a recall score of 100%, a specificity score of 99.79%, and an F1 score of 99.89%. Figure 6 displays the ROC-AUC curve for the proposed methodology. The MGWO-CNN had the highest AUC score of 99.0% compared with the standard GWO with 95.1% AUC score.

Table 1.
Evaluation of the Model.

Evaluation Measures	GWO-CNN	MGWO-CNN
Accuracy (%)	99.48	99.89
Error Rate (%)	0.52	0.11
Sensitivity (%)	99.92	100
Specificity (%)	99.08	99.79
False Positive Rate (%)	0.0092	0.0021
Precision (%)	99.01	99.79
F1-score (%)	99.46	99.89
Execution Time	120mins 43secs	3023mins 01secs

5. Conclusion

The use of chest X-ray pictures, namely those depicting individuals with COVID-19 and those representing healthy individuals, primarily examined pulmonary issues. This investigation analyses the distinct advantages and limitations of the CNN DL model when combined with GWO and MGWO algorithms. The objective is to accurately detect and classify cases of COVID-19 with a satisfactory level of accuracy. Considering the advantages and downsides is crucial for a doctor's decision-making process to make informed choices. Moreover, when there are limitations on time, re-sources, and the patient's health, the physician could be compelled to decide relying only on a single modality. This study used deep learning methodologies to facilitate the automated identification of COVID-19 via the analysis of chest X-ray scans.

The system capabilities were strengthened by including the MGWO in the CNN model. Compared to all other relevant functions, the recommended approach demonstrated exceptional accuracy in categorization. The MGWO-CNN model showed a high level of accuracy, with a rate of 99.89%. The GWO-CNN model achieved a slightly lower accuracy rate of 99.48%.

In further research endeavours, applying the suggested methodology to a dataset including a broader range of respiratory disorders, including but not limited to asthma, lung cancer, and COVID-19, is recommended. Furthermore, the literature analysis revealed inadequate methodologies for extracting features from picture data. Hence, it is essential to include a feature extraction strategy in the next research endeavours.

Transparency:

The authors confirm that the manuscript is an honest, accurate, and transparent account of the study; that no vital features of the study have been omitted; and that any discrepancies from the study as planned have been explained. This study followed all ethical practices during writing.

Copyright:

References

[1] P. Rai, B. K. Kumar, V. K. Deekshit, I. Karunasagar, and I. Karunasagar, "Detection technologies and recent developments in the diagnosis of COVID-19 infection," *Applied Microbiology and Biotechnology*, vol. 105, pp. 441-455, 2021, doi: https://doi.org/10.1007/s00253-020-11061-5.

[2] R. O. Ogundokun, A. F. Lukman, G. B. Kibria, J. B. Awotunde, and B. B. Aladeitan, "Predictive modelling of COVID-19 confirmed cases in Nigeria," *Infectious Disease Modelling*, vol. 5, pp. 543-548, 2020, doi: https://doi.org/10.1016/j.idm.2020.08.003.

[3] M. O. Arowolo, R. O. Ogundokun, S. Misra, B. D. Agboola, and B. Gupta, "Machine learning-based IoT system for COVID-19 epidemics," *Computing*, vol. 105, no. 4, pp. 831-847, 2023, doi: https://doi.org/10.1007/s00607-022-01057-6.

[4] ECDC, "COVID-19 situation update worldwide," European centre for disease prevention and control," 2020. [Online]. Available: https://www.ecdc.europa.eu/en/covid-19/situation-updates

[5] M. Cascella, M. Rajnik, A. Aleem, S. Dulebohn, and R. Di Napoli, "Features, evaluation, and treatment of coronavirus (COVID-19)," StatPearls," 2023. [Online]. Available: https://www.ncbi.nlm.nih.gov/books/NBK554776/

[6] American College of Radiology, "Recommendations for the use of chest radiography and computed tomography (CT) for suspected COVID-19 infection," ACR position statement," 2020. [Online]. Available: https://www.acr.org/Advocacy-and-Economics/ACR-Position-Statements/Recommendations-for-Chest-Radiography-and-CT-for-Suspected-COVID19-Infection

[7] H. Y. F. Wong *et al.*, "Frequency and distribution of chest radiographic findings in patients positive for COVID-19," *Radiology*, vol. 296, no. 2, pp. E72-E78, 2020, doi: https://doi.org/10.1148/radiol.2020201160.

[8] S. Cho *et al.*, "Enhancement of soft-tissue contrast in cone-beam CT using an anti-scatter grid with a sparse sampling approach," *Physica Medica*, vol. 70, pp. 1-9, 2020.

[9] J. Fu, J. Wang, W. Guo, and P. Peng, "Multi-mounted X-ray cone-beam computed tomography," *Nuclear Instruments and Methods in Physics Research Section A*, vol. 888, pp. 119–125, 2018, doi: https://doi.org/10.1016/j.nima.2018.01.074.

[10] P. M. Shakeel, M. Burhanuddin, and M. I. Desa, "Automatic lung cancer detection from CT image using improved deep neural network and ensemble classifier," *Neural Computing and Applications*, pp. 1-14, 2022.

[11] K. Ye, Q. Zhu, M. Li, Y. Lu, and H. Yuan, "A feasibility study of pulmonary nodule detection by ultralow-dose CT with adaptive statistical iterative reconstruction-V technique," *European Journal of Radiology*, vol. 119, p. 108652, 2019.

[12] N. Maleki, Y. Zeinali, and S. T. A. Niaki, "A k-NN method for lung cancer prognosis with the use of a genetic algorithm for feature selection," *Expert Systems with Applications*, vol. 164, p. 113981, 2021.

[13] Q. Al-Tashi, S. J. A. Kadir, H. M. Rais, S. Mirjalili, and H. Alhussian, "Binary optimization using hybrid grey wolf optimization for feature selection," *Ieee Access*, vol. 7, pp. 39496-39508, 2019.

[14] F. A. Şenel, F. Gökçe, A. S. Yüksel, and T. Yiğit, "A novel hybrid PSO–GWO algorithm for optimization problems," *Engineering with Computers*, vol. 35, pp. 1359-1373, 2019.

[15] S. H. S. Moosavi and V. K. Bardsiri, "Satin bowerbird optimizer: A new optimization algorithm to optimize ANFIS for software development effort estimation," *Engineering Applications of Artificial Intelligence*, vol. 60, pp. 1-15, 2017.

[16] D. Simon, "Biogeography-based optimization," *IEEE Transactions on Evolutionary Computation*, vol. 12, no. 6, pp. 702-713, 2008.

[17] G. Yildizdan and Ö. K. Baykan, "A novel modified bat algorithm hybridizing by differential evolution algorithm," *Expert Systems with Applications*, vol. 141, p. 112949, 2020.

[18] F. MiarNaeimi, G. Azizyan, and M. Rashki, "Horse herd optimization algorithm: A nature-inspired algorithm for high-dimensional optimization problems," *Knowledge-Based Systems*, vol. 213, p. 106711, 2021.

[19] M. Ragab, S. Alshehri, N. A. Alhakamy, R. F. Mansour, and D. Koundal, "Multiclass classification of chest x-ray images for the prediction of covid-19 using capsule network," *Computational Intelligence and Neuroscience*, vol. 2022, no. 1, p. 6185013, 2022.

[20] E. Ranschaert, L. Topff, and O. Pianykh, "Optimization of radiology workflow with artificial intelligence," *Radiologic Clinics*, vol. 59, no. 6, pp. 955-966, 2021.

[21] S. Anjum *et al.*, "Detecting brain tumors using deep learning convolutional neural network with transfer learning approach," *International Journal of Imaging Systems and Technology*, vol. 32, no. 1, pp. 307-323, 2022.

[22] X. Zhang, J. Zou, K. He, and J. Sun, "Accelerating very deep convolutional networks for classification and detection," *IEEE transactions on pattern analysis and machine intelligence*, vol. 38, no. 10, pp. 1943-1955, 2015.

[23] Z. Chen, J. Wu, J. Hou, L. Li, W. Dong, and G. Shi, "ECSNet: Spatio-temporal feature learning for event camera," *IEEE Transactions on Circuits and Systems for Video Technology*, vol. 33, no. 2, pp. 701-712, 2022.

[24] H. Zaidi and I. El Naqa, "Quantitative molecular positron emission tomography imaging using advanced deep learning techniques," *Annual Review of Biomedical Engineering*, vol. 23, no. 1, pp. 249-276, 2021.

[25] K. Zhou *et al.*, "Eleven routine clinical features predict COVID-19 severity uncovered by machine learning of longitudinal measurements," *Computational and structural biotechnology journal*, vol. 19, pp. 3640-3649, 2021.

[26] V. Gupta and V. Bibhu, "Deep residual network based brain tumor segmentation and detection with MRI using improved invasive bat algorithm," *Multimedia Tools and Applications*, vol. 82, no. 8, pp. 12445-12467, 2023.
[27] S. Lu, S.-H. Wang, and Y.-D. Zhang, "Detection of abnormal brain in MRI via improved AlexNet and ELM optimized by chaotic bat algorithm," *Neural Computing and Applications*, vol. 33, no. 17, pp. 10799-10811, 2021.
[28] N. Dey and V. Rajinikanth, *Applications of bat algorithm and its variants*. Springer, 2021.
[29] M. A. Kassem, K. M. Hosny, R. Damaševičius, and M. M. Eltoukhy, "Machine learning and deep learning methods for skin lesion classification and diagnosis: a systematic review," *Diagnostics*, vol. 11, no. 8, p. 1390, 2021.
[30] J. Islam and Y. Zhang, "Early diagnosis of Alzheimer's disease: A neuroimaging study with deep learning architectures," in *In Proc. IEEE Conf. Comput. Vis. Pattern Recognit. Workshops (CVPRW), pp. 1881–1883*, 2018.
[31] D. Eldred-Evans *et al.*, "The rapid assessment for prostate imaging and diagnosis (RAPID) prostate cancer diagnostic pathway," *BJU international*, vol. 131, no. 4, pp. 461-470, 2023.
[32] B. Nithya and V. Ilango, "Evaluation of machine learning based optimized feature selection approaches and classification methods for cervical cancer prediction," *SN Applied Sciences*, vol. 1, pp. 1-16, 2019.
[33] B. Gayathri, C. Sumathi, and T. Santhanam, "Breast cancer diagnosis using machine learning algorithms-a survey," *International Journal of Distributed and Parallel Systems*, vol. 4, no. 3, p. 105, 2013.
[34] I. U. Khan and N. Aslam, "A deep-learning-based framework for automated diagnosis of COVID-19 using X-ray images," *Information*, vol. 11, no. 9, p. 419, 2020.
[35] M. Nour, Z. Cömert, and K. Polat, "A novel medical diagnosis model for COVID-19 infection detection based on deep features and Bayesian optimization," *Applied Soft Computing*, vol. 97, p. 106580, 2020.
[36] M. E. Chowdhury *et al.*, "Can AI help in screening viral and COVID-19 pneumonia?," *Ieee Access*, vol. 8, pp. 132665-132676, 2020.
[37] S. Asif, Y. Wenhui, H. Jin, Y. Tao, and S. Jinhai, "Automatic detection of COVID-19 using X-ray images with deep convolutional neural networks and machine learning," 2020.
[38] M. Toğaçar, B. Ergen, and Z. Cömert, "COVID-19 detection using deep learning models to exploit Social Mimic Optimization and structured chest X-ray images using fuzzy color and stacking approaches," *Computers in biology and medicine*, vol. 121, p. 103805, 2020.
[39] F. Ucar and D. Korkmaz, "COVIDiagnosis-Net: Deep Bayes-SqueezeNet based diagnosis of the coronavirus disease 2019 (COVID-19) from X-ray images," *Medical hypotheses*, vol. 140, p. 109761, 2020.
[40] A. Jaiswal and A. Bist, "Analysis of deep learning algorithms on COVID-19 radiography database," *International Journal of Advanced Science and Technology*, vol. 29, no. 11, pp. 1268-1275, 2020.
[41] T. Ozturk, M. Talo, E. A. Yildirim, U. B. Baloglu, O. Yildirim, and U. R. Acharya, "Automated detection of COVID-19 cases using deep neural networks with X-ray images," *Computers in biology and medicine*, vol. 121, p. 103792, 2020.
[42] M. Canayaz, S. Şehribanoğlu, R. Özdağ, and M. Demir, "COVID-19 diagnosis on CT images with Bayes optimization-based deep neural networks and machine learning algorithms," *Neural Computing and Applications*, vol. 34, no. 7, pp. 5349-5365, 2022, doi: https://doi.org/10.1007/s00521-022-07052-4.
[43] R. C. Junia and K. Selvan, "Deep learning-based automatic segmentation of COVID-19 in chest X-ray images using ensemble neural net sentinel algorithm," *Measurement: Sensors*, vol. 33, p. 101117, 2024.
[44] X. Kong *et al.*, "Real-time mask identification for COVID-19: An edge-computing-based deep learning framework," *IEEE Internet of Things Journal*, vol. 8, no. 21, pp. 15929-15938, 2021.
[45] A. Dash and T. Swarnkar, "CoVaD-GAN: An efficient data augmentation technique for covid cxr image classification," presented at the In 2023 2nd International Conference on Ambient Intelligence in Health Care (ICAIHC) (pp. 1-7), 2023.
[46] S. Mirjalili, S. M. Mirjalili, and A. Lewis, "Grey wolf optimizer," *Advances in Engineering Software*, vol. 69, pp. 46-61, 2014.
[47] P. Hu, J. S. Pan, and S. C. Chu, "Improved binary grey wolf optimizer and its application for feature selection," *Knowl. Based Syst*, vol. 195, p. 105746, 2020.

Edelweiss Applied Science and Technology
ISSN: 2576-8484
Vol. 9, No. 4: 379-394, 2025
DOI: 10.55214/25768484.v9i4.5993